

# Dissecting the *Spitzer* color-magnitude diagrams of extreme LMC AGB stars

F. Dell’Agli<sup>1,2</sup>, P. Ventura<sup>1</sup>, D. A. García Hernández<sup>3,4</sup>, R. Schneider<sup>1</sup>,  
M. Di Criscienzo<sup>1</sup>, E. Brocato<sup>1</sup>, F. D’Antona<sup>1</sup>, C. Rossi<sup>2</sup>

<sup>1</sup>INAF – Osservatorio Astronomico di Roma, Via Frascati 33, 00040, Monte Porzio Catone (RM), Italy

<sup>2</sup>Dipartimento di Fisica, Università di Roma “La Sapienza”, P.le Aldo Moro 5, 00143, Roma, Italy

<sup>3</sup>Instituto de Astrofísica de Canarias, Vía Láctea s/n, E-38200 La Laguna, Tenerife, Spain

<sup>4</sup>Dept. Astrofísica, Universidad de La Laguna (ULL), E-38206 La Laguna, Tenerife, Spain

Accepted, Received; in original form

## ABSTRACT

We trace the full evolution of low- and intermediate-mass stars ( $1M_{\odot} \leq M \leq 8M_{\odot}$ ) during the Asymptotic Giant Branch (AGB) phase in the *Spitzer* two-color and color-magnitude diagrams. We follow the formation and growth of dust particles in the circumstellar envelope with an isotropically expanding wind, in which gas molecules impinge upon pre-existing seed nuclei, favour their growth. These models are the first able to identify the main regions in the *Spitzer* data occupied by AGB stars in the Large Magellanic Cloud (LMC). The main diagonal sequence traced by LMC extreme stars in the [3.6]-[4.5] vs. [5.8]-[8.0] and [3.6]-[8.0] vs. [8.0] planes are nicely fit by carbon stars models; it results to be an evolutionary sequence with the reddest objects being at the final stages of their AGB evolution. The most extreme stars, with  $[3.6] - [4.5] > 1.5$  and  $[3.6] - [8.0] > 3$ , are  $2.5 - 3M_{\odot}$  stars surrounded by solid carbon grains. In higher mass ( $> 3M_{\odot}$ ) models dust formation is driven by the extent of Hot Bottom Burning (HBB) - most of the dust formed is in the form of silicates and the maximum obscuration phase by dust particles occurs when the HBB experienced is strongest, before the mass of the envelope is considerably reduced.

**Key words:** Stars: abundances – Stars: AGB and post-AGB. ISM: abundances, dust

## 1 INTRODUCTION

A reliable estimate of the nature and the amount of dust produced by Asymptotic Giant Branch (AGB) stars proves essential for a number of scientific issues. These stars are believed to be the dominant stellar sources of dust in the present-day Universe and their contribution to dust enrichment can not be neglected even at redshift  $z > 6$  (Valiante et al. 2011). In order to properly include their contribution in chemical evolution models with dust, the mass and composition of dust grains released by each star as a function of its mass and metallicity need to be known. In addition, the corresponding size distribution function allows to compute the extinction properties associated with these grains, which is fundamental information required for correctly interpreting the optical-near infrared properties of high- $z$  quasar and gamma ray burst spectra (Gallerani et al. 2010).

Theoretical modelling of dust formation around AGBs has made considerable steps forward in the last years, owing to the pioneering explorations by the Heidelberg group (see e.g. Ferrarotti & Gail 2006, and references therein),

complemented by recent studies (Ventura et al. 2012a,b; Di Criscienzo et al. 2013; Ventura et al. 2014; Nanni et al. 2013, 2014). The reliability of these models must be tested against the observations, given the many uncertainties affecting the AGB phase modelling (see e.g. Herwig 2005), and the description of the formation and growth of dust grains in the winds of AGBs (Ferrarotti & Gail 2006).

On the observational side, the study of evolved stars in the Galaxy is hampered by the obscuration determined by the interstellar medium, and by the unknown distances of the objects observed. This pushed the interest towards other nearby galaxies. The Large Magellanic Cloud (LMC) is an optimum target for this scope. This stems from the low average reddening ( $E(B - V) \sim 0.075$ ) and its proximity, that allows the determination of important stellar properties, such as the absolute magnitudes. The LMC has been surveyed in the optical by the Magellanic Clouds Photometric Survey (MCPS, Zaritsky et al. 1997), in the near-IR by the Deep Near Infrared Survey of the Southern Sky (DENIS, Epchtein et al. 1994) and the Two Micron All Sky Survey (2MASS, Skrutskie et al. 2006). Of particular interest for the study of evolved, dust-surrounded stars, is the

SAGE (Surveying the Agents of Galaxy Evolution) survey obtained by the *Spitzer Space Telescope* with the Infrared Array Camera (IRAC; 3.6, 4.5, 5.8 and 8.0  $\mu\text{m}$ ) and the Multiband Imaging Photometer for *Spitzer* (MIPS; 24, 70 and 160  $\mu\text{m}$ ) (see e.g. Meixner et al. 2006). The analysis of evolved stars based on 2MASS and IRAC data lead to a classification of LMC stars into three main categories. Cioni et al. (2006), based on their analysis of the 2MASS color-magnitude diagram (CMDs), divided the region above the tip of the Red Giant Branch (RGB) into O-rich and C-rich zones; Blum et al. (2006) selected a group of stars, called “extreme”, showing the clear signature of the presence of a dusty circumstellar envelope. These stars were shown to contribute about 75% of the overall dust from AGBs (Riebel et al. 2012). This stimulated an interesting series of papers (Srinivasan et al. 2009; Sargent et al. 2011; Srinivasan et al. 2011; Boyer et al. 2011) aimed at refining such a classification, to interpret the observed CMDs by using grids of synthetic spectra for various chemical and physical inputs, the most relevant being the surface chemistry of the star, the size of the grains formed, the borders of the dusty shell, the surface gravity and the effective temperature of the central object.

In this Letter we use models of dust formation around AGBs, based on full evolutionary computations, to interpret the distribution of LMC extreme stars in the color–color and color–magnitude diagrams (CCDs and CMDs, respectively). Our goal is to characterize the extreme stars in terms of the evolutionary phase, and of the amount and type of dust present in their surroundings. This investigation will be an important benchmark for the studies focused on dust formation around AGB stars.

## 2 STELLAR EVOLUTION AND DUST FORMATION MODELLING

The evolutionary sequences have been calculated by means of the ATON code for stellar evolution. The interested reader may find the details of the numerical structure of the code together with the more recent updates in Ventura & D’Antona (2009). The range of masses investigated is  $1M_{\odot} \leq M \leq 8M_{\odot}$ . More massive stars undergo core collapse by e-capture, and do not experience the AGB phase. Models with  $6.5M_{\odot} < M < 8M_{\odot}$  achieve carbon ignition in conditions of partial degeneracy, and develop a core made up of oxygen and neon; their phase of thermal pulses is commonly known as super-AGB (hereafter SAGB, Siess 2006). We assumed a chemical composition typical for LMC stars:  $Z = 0.008$ ,  $Y = 0.26$ .

We recall here the physical inputs most relevant to the results obtained. The convective instability is treated according to the Full Spectrum of Turbulence (FST) description, developed by Canuto & Mazzitelli (1991); in models whose initial mass exceeds  $\sim 3M_{\odot}$ , use of the FST model leads to strong Hot Bottom Burning (HBB, Renzini & Voli 1981) conditions, with the activation of an advanced p-capture nucleosynthesis at the bottom of the convective envelope (Ventura & D’Antona 2005). Mass loss for M-stars is modelled following Blöcker (1995); for carbon stars, we use the results by Wachter et al. (2008). In regions unstable to convective motions, nuclear burning and mixing of chem-

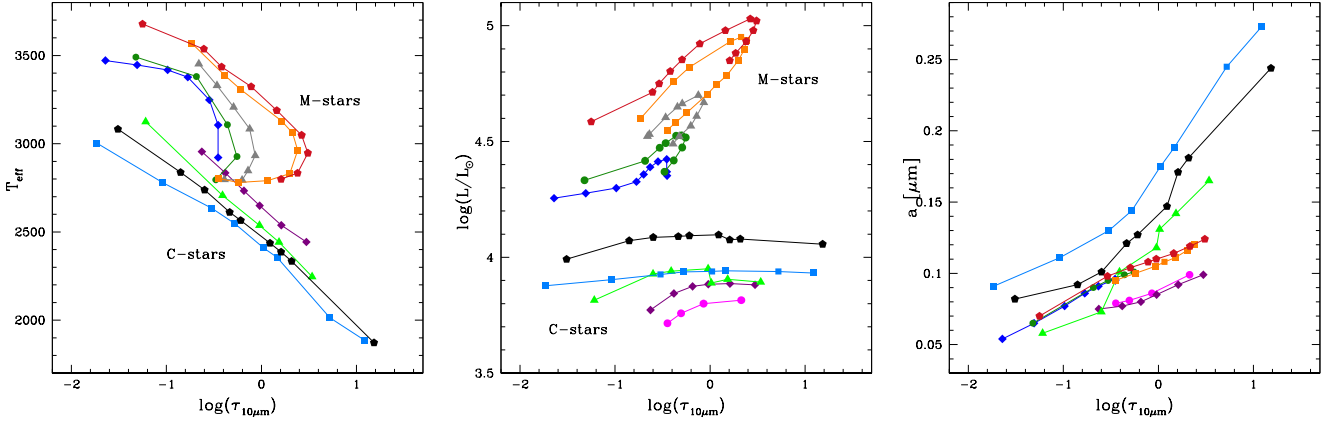
icals are coupled via a diffusive approach, as described in Cloutmann & Eoll (1976); during the AGB phase, convective velocities are allowed to decay exponentially into radiatively stable regions, based on the calibration aimed at reproducing the observed luminosity function of carbon stars, discussed in Ventura et al. (2014). The wind surrounding AGBs is assumed to expand isotropically, and to be accelerated by radiations pressure on dust particles. The growth of dust grains is described by condensation of gas molecules in the wind impinging on the already formed grains. The relevant equations can be found, e.g., in Ferrarotti & Gail (2006), and were already used in other investigations by our group (Ventura et al. 2012a,b; Di Criscienzo et al. 2013; Ventura et al. 2014), and also by Nanni et al. (2013, 2014).

The spectral energy distribution (SED) of the star during the various evolutionary phases was determined from the knowledge of the properties of the central object and of the structure of the dust shell by means of the DUSTY code (Ivezic et al. 1999). For M-stars we considered the presence of amorphous silicates (mainly olivine) and alumina dust grains, whereas solid amorphous carbon and SiC particles were used for C-stars. Iron grains are also accounted for in both cases. In addition, for a given AGB evolutionary time, the location (and temperature) of the inner dust region boundary, the density stratification, the relative percentages of the different dust species (i.e., SiC vs. AmC, Silicates vs. alumina), the optical depth and the dust grain size as calculated self-consistently by our wind AGB models (Ventura et al. 2014 and references therein) are then used as inputs in DUSTY (see Dell’Agli et al., in preparation). Finally, to test the reliability of the results obtained, we calculated a few SEDs with the 2-DUST code (Ueta & Meixner 2003), run in the spherically symmetric mode. The location of the various dusty layers and the relative percentages of the dust species present are assumed consistently with the results from the wind modelling. These tests showed no differences ( $<10\%$  in flux) among the results obtained with the two codes.

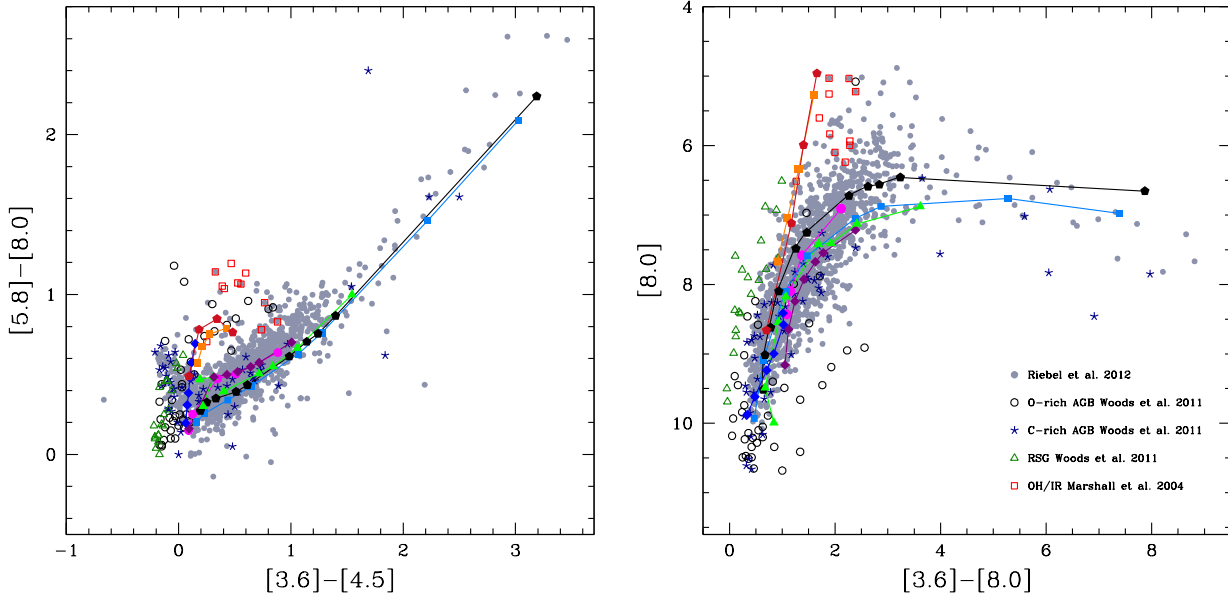
## 3 DUST FORMATION DURING THE AGB PHASE

Fig. 1 shows the evolution of models of different mass during the AGB phase. Because this work is focused on the most obscured objects, we restrict our analysis to stars that have already reached the C-star stage, or M-stars where HBB is active; these are the only conditions allowing dust production in meaningful quantities. We show the variation of the effective temperature, luminosity and size of the grains formed as a function of the optical depth at 10  $\mu\text{m}$  ( $\tau_{10\mu\text{m}}$ ), which quantifies the degree of obscuration of the central star. It is not possible to define a unique grain size, because particles of various species form, with different dimensions: here we refer to the grains that dominate the dust mass formed, providing most of the acceleration of the wind by radiation pressure, i.e. solid carbon for C-stars and olivine for M-stars (Ferrarotti & Gail 2006).

The evolution of C-stars is driven by the carbon enrichment at the surface, favoured by the occurrence of Third Dredge Up (TDU). As the surface of the star becomes more enriched in carbon, the star assumes a more extended



**Figure 1.** The evolution of AGB models of various mass shown as a function of  $\tau_{10\mu\text{m}}$ , indicating the degree of obscuration. The panels show the variation of the effective temperature (left panel), luminosity (middle) and size of the grains formed (right); we refer to olivine for M-stars, and solid carbon for C-stars). The meaning of the symbols is as follows. Magenta circles:  $1.25M_{\odot}$ ; violet diamonds:  $1.5M_{\odot}$ ; light green triangles:  $2M_{\odot}$ ; light blue squares:  $2.5M_{\odot}$ ; black pentagons:  $3M_{\odot}$ ; blue diamonds:  $3.5M_{\odot}$ ; green circles:  $4M_{\odot}$ ; grey triangles:  $5M_{\odot}$ ; orange squares:  $6.5M_{\odot}$ ; red pentagons:  $7.5M_{\odot}$ .



**Figure 2.** Data of LMC extreme stars taken from Riebel et al. (2012) are shown as solid, grey circles in the  $[3.6] - [4.5]$  vs  $[5.8] - [8.0]$  (left) and  $[3.6] - [8.0]$  vs  $[8.0]$  (right) diagrams. The position of the models during the AGB evolution are also shown (colors are the same as in Fig. 1). Spectroscopically confirmed C- and O-rich AGBs and RSG stars (from Woods et al. 2011) as well as extreme OH/IR stars (from Marshall et al. 2004) are also marked with different symbols/colors in these diagrams.

configuration (Marigo 2002; Ventura & Marigo 2009, 2010), evolves towards lower effective temperatures ( $T_{\text{eff}}$ ) and loses mass at larger rates (Wachter et al. 2008): all these factors favour dust production, mainly under the form of solid carbon, with traces of SiC and iron (Ferrarotti & Gail 2006). We see in the left panel of Fig. 1 that the stars become more and more obscured as the external layers cool; C-stars with the same  $T_{\text{eff}}$  have the same degree of obscuration, independent of their previous history. The most obscured stars, with  $\tau_{10\mu\text{m}} \sim 10$ , are those in the final stages of the AGB evolution, when the size of the carbon grains is

$a_C \sim 0.20 - 0.25\mu\text{m}$  (Ventura et al. 2014; Nanni et al. 2013). The middle panel of Fig. 1 shows that the luminosity has only a minor effect on the optical depth variation of C-stars; higher mass stars evolve at larger luminosities, owing to their larger core masses. We note that these optical depth (and luminosity) values are consistent with those derived for the most extreme C-stars in the LMC (Gruendl et al. 2008).

Stars with initial mass above  $3M_{\odot}$  experience HBB, that prevents the possibility of reaching the C-star stage; their evolution is driven by the temperature at the bottom of the envelope, which determines the luminosity, the mass-

loss rate and consequently the quantity of dust formed. As shown in the middle panel of Fig. 1, the luminosity ( $L$ ) undergoes significant variations during the AGB evolution: after the initial increase, due to the growth of the core mass,  $L$  decreases, owing to the gradual loss of the external mantle. The phase of maximum dust production (with the highest  $\tau_{10\mu\text{m}}$ ) is in conjunction with the maximum  $L$ , when the mass–loss rate also attains its largest values. Note that  $L$  in extreme OH/IRs ( $10^4 - 10^5 L_\odot$ ; Marshall et al. 2004) agrees very well with our predictions for the more massive AGBs. Stars in the SAGB regime, owing to their large core mass, reach the highest values of  $\tau_{10\mu\text{m}}$ , that approaches  $\sim 3$  in the  $7.5M_\odot$  model. The right panel of Fig. 1 shows the tight relationship between the size of the olivine grains ( $a_{\text{ol}}$ ) formed and  $\tau_{10\mu\text{m}}$ ;  $a_{\text{ol}}$  changes from  $\sim 0.1\mu\text{m}$  to  $\sim 0.13\mu\text{m}$  as  $\tau_{10\mu\text{m}}$  grows from 1 to  $\sim 3$ . In the high-mass domain the  $T_{\text{eff}}$  has a minor effect on  $\tau_{10\mu\text{m}}$ , in agreement with the fact that dust production is mostly determined by the extent of the HBB experienced. The narrow  $T_{\text{eff}}$  range ( $2700 < T_{\text{eff}} < 3500$  K) predicted in the more massive AGB stars agree quite well with the spectroscopic temperatures derived for such stars in the LMC (García-Hernández et al. 2009) and our own Galaxy (García-Hernández et al. 2006, 2007)<sup>1</sup>.

#### 4 THE INTERPRETATION OF THE EXTREME STARS IN THE LMC

The *Spitzer* data of extreme stars in the LMC from Riebel et al. (2012) are shown in the two panels of Fig. 2. We also display the smaller group of spectroscopically confirmed C- and O-rich AGBs (and luminous red supergiants, RSGs) from Woods et al. (2011) as well as the small sample of extreme OH/IR stars from Marshall et al. (2004)<sup>2</sup>. The position of our models during different stages of the AGB phase are also indicated.

In the  $[5.8] - [8.0]$  vs.  $[3.6] - [4.5]$  plane the theoretical models of C-stars define a diagonal sequence, that nicely fits the observed colors. We interpret the reddest objects, with  $[3.6] - [4.5] > 1.5$ , as the latest evolutionary stages of stars of initial mass  $\sim 2.5 - 3M_\odot$ , just below the threshold to ignite HBB. These are the only progenitor masses in which the surface C reaches abundances  $X(C) \sim 0.01$ , with a great production of carbon dust, provoking a strong obscuration of the central star. We expect that only a few stars populate this region, as confirmed by the observations.

The observed spread in  $[5.8] - [8.0]$  for a given value of  $[3.6] - [4.5]$  is due to the different relative distribution of SiC and carbon dust. Models with a high SiC/C ratio exhibit a more prominent feature at  $11.3\mu\text{m}$ , and will be less obscured, particularly in the  $[3.6] - [4.5]$  color. This is the case of stars with mass  $M \leq 1.5M_\odot$ , that will populate the upper region in the color-color plane at  $[3.6] - [4.5] < 1.5$ . Strong production of carbon dust limits the formation of SiC, owing to the strong acceleration of the wind. Therefore, the stars whose SED exhibits the most pronounced feature of SiC are

those of initial mass below  $\sim 2M_\odot$ , in which the surface C abundance keeps below  $X(C) \sim 0.01$ . More massive models ( $M \sim 2.5 - 3M_\odot$ ) achieve extremely high surface C abundances. In the latest AGB phases, these models evolve at  $[3.6] - [4.5] > 1.5$  and the SED is characterized by the appearance of a weak absorption SiC feature at  $11.3\mu\text{m}$ . Thus, our finding confirms the interpretation/observations of the LMC “extremely red objects” by Gruendl et al. (2008).

C-stars models also fit the observed *Spitzer* CMD. The observed spread in the  $8\mu\text{m}$  flux is a luminosity effect; higher mass stars evolve on more massive cores, thus at larger luminosities (see middle panel of fig. 1), and smaller  $[8.0]$  magnitudes. In both panels of Fig.2 we see that the position of the spectroscopically confirmed C-rich AGBs by Woods et al. (2011) is nicely reproduced by our models. The only exception is the group of objects at  $[3.6] - [4.5] < 0$ , representing the C-stars with little (if any) dust in their envelopes. Their *Spitzer* colors and magnitudes are reproduced by the dust-free photosphere models by Aringer et al. (2009).

AGB stars experiencing HBB trace a different path. As shown in fig. 1, these stars evolve at smaller optical depths compared to C-stars, because the extinction coefficient of carbon dust exceeds that of silicates. In the CCD, the theoretical tracks are confined in the region  $[3.6] - [4.5] < 0.5$ . The slope of the line traced by the theoretical tracks is different from that traced by C-stars; this is because the strong silicates feature determines a great increase in the  $8\mu\text{m}$  flux, with a considerable increase in the  $[5.8] - [8.0]$  color.

Massive AGBs with  $M > 6M_\odot$  evolve at  $\tau_{10\mu\text{m}} > 2$  (see fig. 1), and populate the region at  $[5.8] - [8.0] > 0.5$ . Unlike their lower mass counterparts, the reddest colors are not reached in the final stages of the AGB evolution, but during the phase of maximum luminosity, when the HBB experienced is strongest. In the CMD, most of the M-stars populate the regions at  $[3.6] - [8.0] < 1$ , and mix with the C-stars. The two sequences bifurcate at  $[8.0] \sim 8$ , because the sequence of massive AGBs, owing to the effects of the silicates feature, trace a steep diagonal line, up to  $[8.0] \sim 5$ . Interestingly, the extreme LMC OH/IR stars (very massive AGBs) are located at the highest  $[8.0]$  magnitudes in good agreement with our massive models; indeed the four OH/IR stars closer to the model predictions are confirmed very massive Rb-rich LMC AGBs (García-Hernández et al. 2009). Models of mass above  $6M_\odot$  experience strong HBB, and evolve at luminosities above the classic limit for AGBs,  $L \sim 5 \times 10^4 L_\odot$  (i.e.  $M_{\text{bol}} = -7.1$ ).

In short, our interpretation of the extreme stars in the LMC is in good agreement with the observations of spectroscopically confirmed C- and O-rich LMC AGBs by Woods et al. (2011). The only difference is in the identification of high luminosity stars with  $[8.0] \sim 5 - 6$ , that we interpret as massive AGBs experiencing strong HBB, whereas Woods et al. (2011) identify as RSGs. Our work suggests that RSGs may be distinguished from massive AGBs/SAGBs in the CMD *Spitzer* diagram but not in the CCD one (see Fig. 2); indeed a small fraction of RSGs may be truly massive AGBs/SAGBs. The O-rich sample by Woods et al. (2011) is nicely reproduced by our massive AGB models in the two *Spitzer* diagrams (Fig. 2), with the exception of the bluest objects, at  $[3.6] - [4.5] < 0$  that, like their C-rich counterparts, have almost dust-free envelopes.

<sup>1</sup> Note, however, that C-rich AGB stars usually display much lower effective temperatures (e.g. Abia et al. 2001) as our models predict.

<sup>2</sup> These are expected to be the most massive LMC AGB stars (García-Hernández et al. 2009).

## 5 CONCLUSIONS

For the first time, we are able to interpret the *Spitzer* observations of extreme stars in the LMC on the basis of evolutionary models of dusty AGB stars.

We find that the main diagonal sequence traced by the observations in the  $[5.8] - [8.0]$  vs.  $[3.6] - [4.5]$  diagram is an evolutionary sequence of C-stars that become progressively more obscured as their surface layers dredge-up carbon from the stellar interior. We identify the reddest objects, with  $[3.6] - [4.5] > 1.5$ , as the descendants of  $\sim 2.5 - 3M_{\odot}$  stars in the latest evolutionary phases, when they develop an optically thick circumstellar envelope. The distribution of stars in the *Spitzer* CCD is generally determined by the optical depth, but it is also dependent on the relative percentages of carbon and SiC dust formed. Stars with a high SiC/carbon ratio populate the upper region of the diagram. This motivates the spread in  $[5.8] - [8.0]$  observed for  $[3.6] - [4.5] < 1.5$ ; the scatter disappears for more obscured objects, because the dust formed is entirely dominated by solid carbon.

Massive AGBs with  $M > 3M_{\odot}$  experience HBB, which prevents them from becoming C-stars; in their circumstellar envelopes the formation of silicates occurs. The strong feature of silicates at  $9.7\mu\text{m}$  favours a considerable increase in the  $8.0\mu\text{m}$  flux, thus the slope traced by the evolutionary sequences in the *Spitzer* CCD is different from C-stars. Owing to the small extinction coefficients of silicates, M-stars do not reach extremely red colors; most of dusty massive AGBs are confined in the region  $[3.6] - [4.5] < 0.5$ , also populated by C-stars. The most massive AGBs experience a phase of strong HBB, when the production of silicates is strongly enhanced: both in the *Spitzer* CCD and CMD these stars will evolve above the main sequence, where most of the stars are detected.

Follow-up (optical and near-IR) spectroscopic observations of the extreme stars in the LMC will be extremely useful to confirm our analysis.

## ACKNOWLEDGMENTS

The authors are indebted to the anonymous referee for the careful reading of the manuscript and for the detailed and relevant comments, that helped to increase the quality of this work. D.A.G.H. acknowledges support provided by the Spanish Ministry of Economy and Competitiveness under grants AYA-2011-27754 and AYA-2011-29060. P.V. was supported by PRIN MIUR 2011 "The Chemical and Dynamical Evolution of the Milk Way and Local Group Galaxies" (PI: F. Matteucci), prot. 2010LY5N2T. R.S. acknowledges funding from the European Research Council under the European Union's Seventh Framework Programme (FP/2007-2013) / ERC Grant Agreement n. 306476.

## REFERENCES

- Abia C., Busso M., Gallino R., Dominguez I., Straniero O., Isern J., 2001, *ApJ*, 559, 1117
- Aringer, B., Girardi, L., Nowotny, W., Marigo, P., Lederer, M. T. 2009, *A&A*, 503, 913
- Blöcker T., 1995, *A&A*, 297, 727
- Blum R. D. et al., 2006, *AJ*, 132, 2034
- Boyer M. L. et al., 2011, *AJ*, 142, 13
- Canuto V.M.C., Mazzitelli I., 1991, *ApJ*, 370, 295
- Cioni M. R. L., Girardi L., Marigo P., Habing H. J., 2006, *A&A*, 448, 77
- Cloutmann, L., & Eoll, J.G. 1976, *ApJ*, 206, 548
- Di Criscienzo M., Dell'Agli F., Ventura P. et al. 2013, *MNRAS*, 433, 313
- Epchtein N. et al., 1994, *AP&SS*, 217, 3
- Ferrarotti A.D., Gail H.P., 2006, *A&A*, 553, 576
- Gallerani S., Maiolino R., Juarez Y., et al., 2010, *A&A*, 523, A85
- García-Hernández D. A., García-Lario P., Plez B. et al. 2006, *Science*, 314, 1751
- García-Hernández D. A., García-Lario P., Plez B. et al. 2007, *A&A*, 462, 711
- García-Hernández D. A., Manchado A., Lambert D. L. et al. 2009, *ApJ*, 705, L31
- Gruendl, R. A., Chu, Y.-H., Seale, J. P. et al. 2008, *ApJ*, 688, L9
- Herwig F., 2005, *AR&A*, 43, 435
- Ivezic Z., Nenkova M., Elitzur M, 1999, User Manual for DUSTY, Univ. Kentucky Internal rep.
- Marshall, J. R., van Loon, J. Th., Matsuura, M. et al. 2004, *MNRAS*, 355, 1348
- Meixner, M., Gordon, K. D., Indebetouw, R. et al. 2006, *AJ* 132, 2268
- Marigo P., 2002, *A&A*, 387, 507
- Nanni A., Bressan A., Marigo P., Girardi L. 2013, *MNRAS*, 434, 2390
- Nanni A., Bressan A., Marigo P., Girardi L. 2014, *MNRAS*, 438, 2328
- Renzini A., Voli M., 1981, *A&A*, 94, 175
- Riebel, S., Srinivasan S., Sargent, B., Meixner, M. 2012, *ApJ*, 753, 71
- Sargent B. A., Srinivasan S., Meixner M. 2011, *ApJ*, 728, 93
- Siess, L., 2006, *A&A*, 448, 717
- Skrutskie M. F. et al., 2006, *AJ*, 131, 1163
- Srinivasan S. et al., 2009, *AJ*, 137, 4810
- Srinivasan S. et al., 2011, *A&A*, 532, A54
- Ueta T., Meixner M., 2003, *ApJ*, 586, 1338
- Valiante R., Schneider R., Salvadori S., Bianchi S., 2011, *MNRAS*, 416, 1916
- Ventura P., D'Antona F., 2005, *A&A*, 431, 279
- Ventura P., D'Antona F., 2009, *MNRAS*, 499, 835
- Ventura P., Di Criscienzo M., Schneider R. et al. 2012a, *MNRAS*, 420, 1442
- Ventura P., Di Criscienzo M., Schneider R. et al. 2012b, *MNRAS*, 424, 2345
- Ventura P., Dell'Agli F., Schneider R., Di Criscienzo M. et al. 2014, *MNRAS*, 439, 977
- Ventura P., Marigo P., 2009, *MNRAS*, 399, L54
- Ventura P., Marigo P., 2010, *MNRAS*, 408, 2476
- Wachter A., Winters J. M., Schröder K. P., Sedlmayr E., 2008, *A&A*, 486, 497
- Woods P. M. et al., 2011, *MNRAS*, 411, 1597
- Zaritsky D., Harris J., Thompson I., 1997, *AJ*, 114, 1002